

EXPERIMENTAL STUDIES ON THE THERMAL BEHAVIOUR OF A TAPERED ROLLER BEARING ASSEMBLY

Vilmar Arthur Schwarz

Universidade Federal de Itajubá, Instituto de Engenharia Mecânica, Itajubá, MG.
vilmar@unifei.edu.br

Abstract. *The purpose of this paper is to present a description of a twin tapered roller bearing assembly and the measurement systems for carrying out an experimental analysis on the thermal behaviour of the assembly, taking into account mainly the bearing friction torque and the operating temperatures of the shaft, bearings and housing. The results are obtained for a range of rotational speeds and loading conditions. The temperatures of the bearing are taken for the inner and the outer raceways, simultaneously with the guide flange lip/roller and contact.*

Keywords. *tapered roller bearing, friction torque, temperatures, heat generation.*

1. Introduction

Tables and formulae for the estimation of rolling contact bearing service life under a variety of operating conditions are given in bearing manufacturers catalogues. However, predictions of bearing behaviour made by using these basic design guides have often led to unsatisfactory results, particularly when thermal factors are involved.

As requirements of rotational speeds, loads, surrounding temperature, or a combination of these three parameters became more demanding, premature failure of rolling contact bearings arising from temperature effects became increasingly common and led to catastrophic and expensive losses. Examples of these temperature effects are:

a) changes of loading conditions resulting from thermal movement of the assembly components, such as axial expansion of the shaft, or housing, or both.

b) Changes in the bearing clearances owing to differential thermal expansion of the bearing rings and rollers, with concomitant effects on the bearing performance, such as torque increase and the eventual establishment of a "thermal spiral".

The aim of this paper is to present an experimental analysis on heat generation and temperature distribution in a tapered roller bearing housing consisted by two identical tapered roller bearings disposed in the so called back-to-back or indirect mounting, bath lubricated by a SAE 20 oil.

A comprehensive description of the test rig and instrumentation is presented, including the load application/measuring system as well as torque and temperature measurement systems.

For purposes of assessing the steady state spacial temperature distribution throughout the whole bearing assembly an array of chromel/constantan thermocouples is used, each couple being located at convenient points within the shaft, bearing rings and housing. In order to install thermocouples in the bearing rings, spark eroded holes were drilled at the bearing cup (outer ring) from the outer diameter to the outer raceway, without trespassing, leaving about 0.5mm thickness from the raceway. With the same special care, no trespassing holes were drilled from the side to the lip of the guide flange of the bearing inner ring, as well as from the bearing bore to the inner raceway.

Apparently, no attempt has been done to access directly the temperature of the cone rib/larger roller ends contact simultaneously with the inner and outer raceways temperatures. Parker and Signer (1977), by measuring the operating temperatures of the cone outer face, cup outer surface, cone bore (shaft outer surface) together with lubricant inlet and outlet temperatures, showed that direct cone-rib lubrication significantly improves the performance of taper roller bearings at high speeds. For example, at a speed of 10,000 rpm the cone outer face temperature was 34°C lower when direct cone-rib lubrication was used rather than lubrication by impingement only, for the same total oil flow rates. However, they did not measure directly the operating temperatures of the cone-rib/large roller end contact, neither the inner and outer raceways temperatures.

Other papers may be found in the literature, dealing with bearing friction torque in tapered roller bearings, without the measurement of the inner and outer raceways temperatures simultaneously with the guide flange lip temperatures, as follows.

Wren and Moyer (1972), investigated theoretically the lubrication conditions in taper roller bearings, over a wide range of speed, loads, and viscosities. They used EHL point contact theory for analysing the lubrication regime between the roller large end and guide flange, while EHL line contact theory was employed for the lubrication analyses for the rolling contact between the rollers and raceways. They concluded that the thickness of the lubricant film between the large roller end and the guide flange was 1.5 to 3.0 times greater than the corresponding film thicknesses at the raceway contacts. All film thicknesses increased with speed, but decreased with thrust load, and these effects of speed and load on film thicknesses were more preponderant for the oil film established between the roller ends and the guide flange.

The effect of speed on the oil film thickness between roller end and guide flange was indirectly confirmed by measuring the rib-roller end friction torque. This torque decreased substantially with speed. They also demonstrated experimentally that, for normal operating conditions, rib torque is insignificant relative to the total bearing torque.

Cretu, S. et al (1995) carried out an analysis on the dynamic behaviour of tapered roller bearings, including the oil film thicknesses at the inner and outer raceways, roller end/lip contact and bearing friction torque. The results for a 32212 tapered roller bearing, running at 100 rpm and under a 3kN thrust load, showed an oil film thickness at the inner raceway contact varying along the roller length, from about $0.372 \mu\text{m}$ at the smaller end to about $0.41 \mu\text{m}$ at the roller larger end. As for the rib/roller end contact the oil film thickness was greater, and the corresponding calculated friction torque being only about 0.0012 N.m for the range of 0.75 to 0.85 values of the ratio between the spherical roller end and the rib radii. Such a friction torque value is absolutely insignificant as compared to the experimentally obtained total bearing friction torque presented by Cretu, which, for a 3000 rpm rotational speed were about 2.8 N.m and 5.1 N.m, for a SAE 20 oil and a Vactra no.4 oil, respectively.

For a larger tapered roller bearing, Wang et al (1996) obtained theoretical rib/roller end friction torques of about 0.0025 N.m, 0.0015 N.m and 0.0018 N.m for rotational speeds of 1000 rpm, 1500 rpm and 3000 rpm, respectively.

2. The test rig

The experimental work was carried out on a specially instrumented rolling contact bearing test rig which allows the following measurement capabilities:

- a) Bearing loading (radial and axial)
- b) Test-shaft rotational speed
- c) Bearing operating torque
- d) Spatial temperature distributions within bearing components, shaft, housings and at specific points in the bedplate/foundations.

The general arrangement of the test rig is shown in Figs. 1 and 2. Power is supplied to the rig from a 3 HP, electric motor via a hydraulic speed variator unit, allowing continuous speed variation from 0 to 5600 rpm. Vibrations within the test module are kept to a minimum by mounting the test-shaft, bearing housings and the drive units on separated mild steel surface-ground gauge plates of 40mm thickness, these being grouted and bolted to a large concrete foundation block. The whole assembly is isolated from external vibrations by sitting the concrete block on rubber pressure mats.

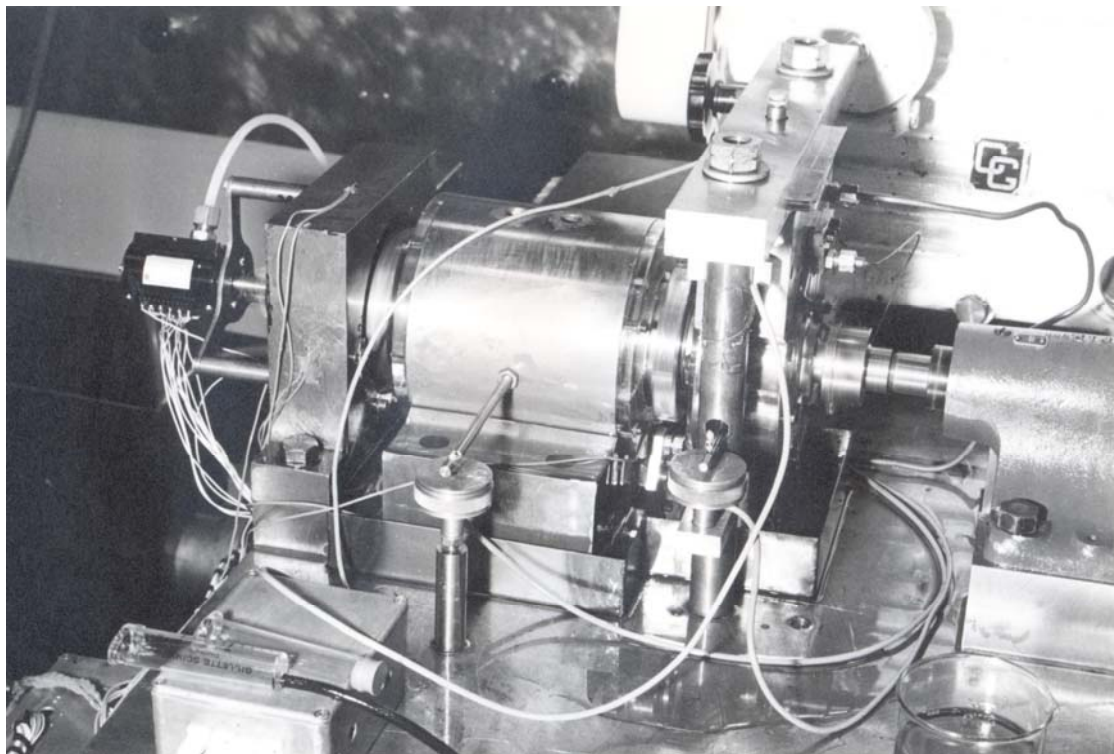


Figure 1. The test rig, showing the load cells, thermocouples and slip-ring unit

As shown in Fig. 2, the test module proper consists essentially of two identical taper roller bearings (11), mounted back-to-back on the test shaft (13) and contained within a cylindrical sleeve (12). The latter rests on a hydrostatic

bearing (14), which applies radial load to the system. A constant oil film thickness is maintained between the loading block (14) (also shown in Figure 3) and the bearing mounting ring (12) by the external oil pressure to the system.

Reaction to the applied load is provided by two identical cylindrical roller bearings (7) fitted onto each end of the test-shaft (13). The forward bearing (7) is mounted in a conventional housing (8) (bolted down to the bedplate) whilst the rear one is carried in the cylindrical sleeve (6) of an inverted hydrostatic system (5). The hydrostatic block (5) is mounted between the rear housing (6) and a horizontal ground steel plate (4), alignment being provided by a hemi cylindrical hydrostatic pad. The horizontal beam (4) is clamped to two pillars (3), which are threaded to the bedplate (2). The twin pillars, therefore, directly react the radial load applied to the rear cylindrical roller bearing.

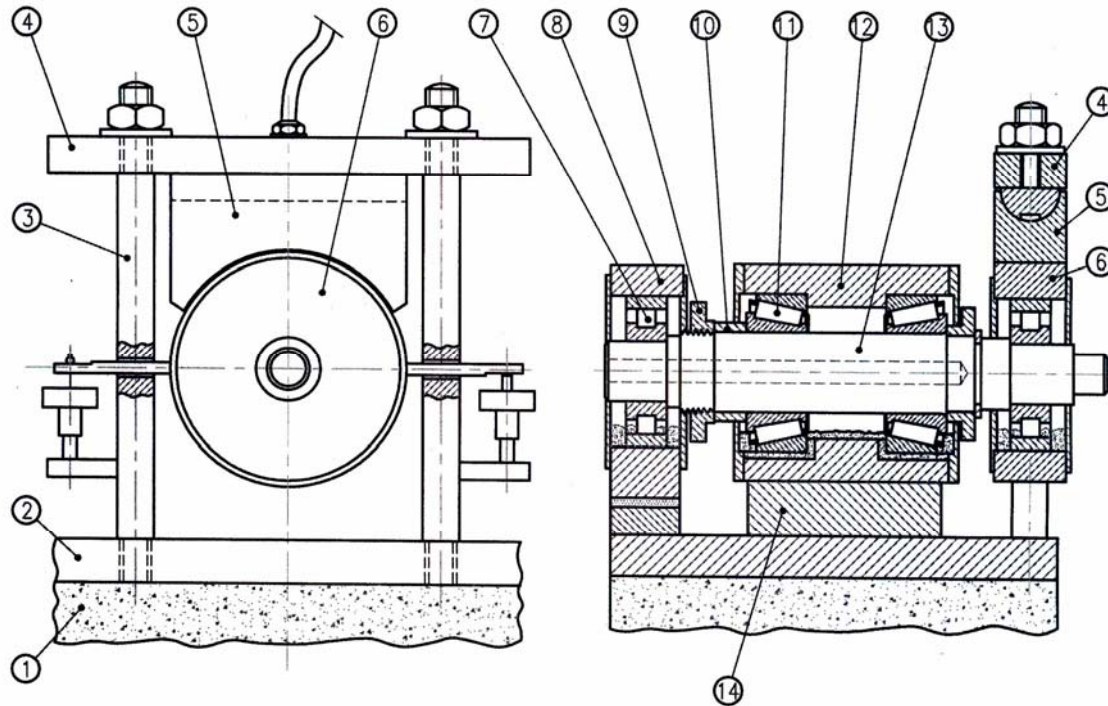


Figure 2. The test module, showing the test shaft and the twin tapered roller bearings



Figure 3. The four pockets hydrostatic block with a partially removed capillary restrictor

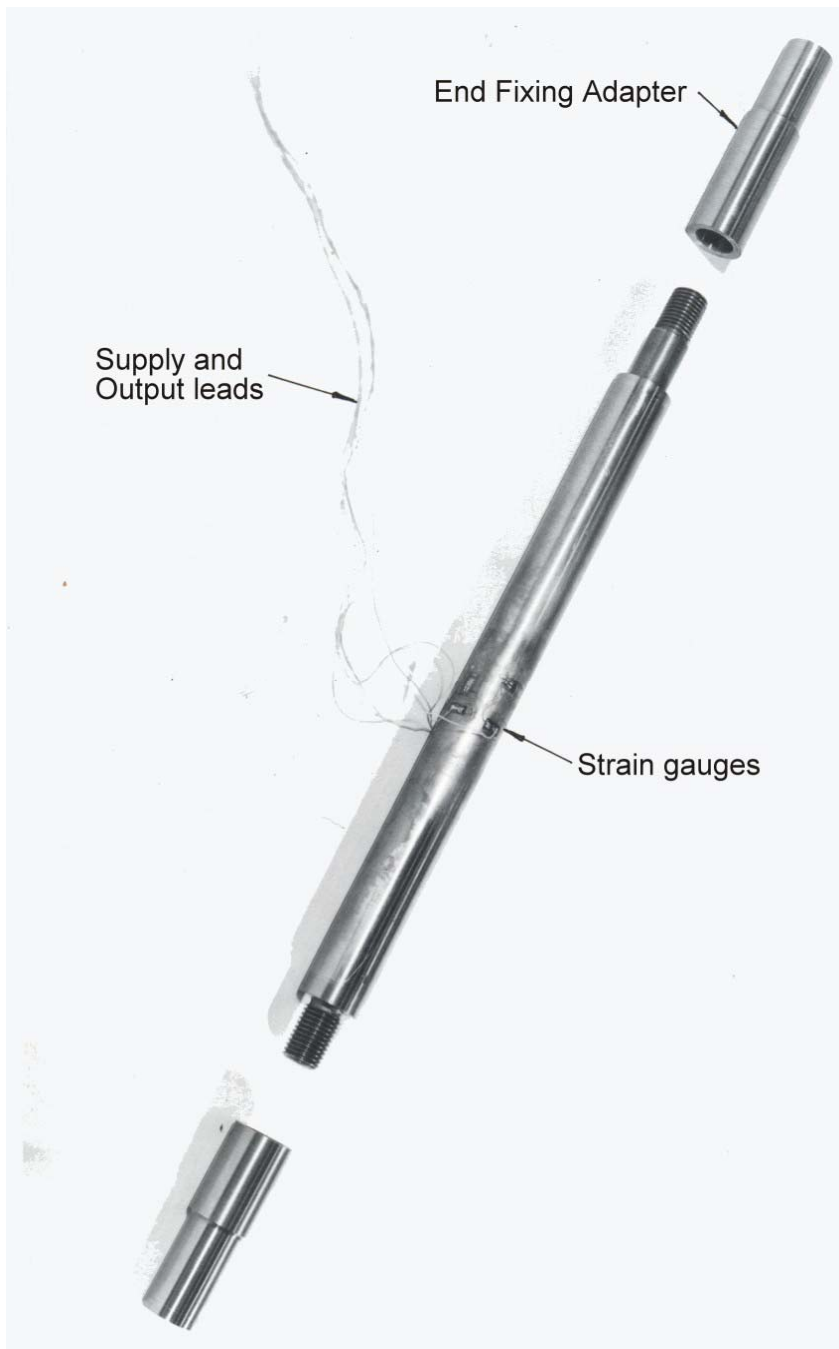
3. The measurement systems

Continuous monitoring of bearing operating torque, applied loads, temperature distribution, and speed was achieved via the following systems.

3.1. Radial load system

Infinitely variable radial loading is applied to the bearing system by means of the hydrostatic oil lift (14), Fig.2. The lift is a four-pocket system, as shown in Fig. 3, applying its load upwards directly to the tapered roller test bearings (11)

mounted in the central sleeve (12), Fig. 2. The applied load is reacted by the front bearing-housing (8) and the inverted hydrostatic oil lift (5). As shown in Fig. 2, the latter hydrostatic system is restrained to move upwards by the horizontal beam (4) and the twin pillars (3) (fixed to the bedplate). Therefore, the radial load applied to the rear roller bearing can easily be assessed by measuring the tensile loads on each pillar. A D.C. activated strain gauge bridge mounted on each pillar (see Fig. 1) measures the tensile load, i.e. the rear roller bearing radial load.



(a) radial load pillar



(b) axial load sensor

Figure 4. Radial load pillar and axial load sensor showing strain gauges.

Four identical strain gauges were bonded to the cylindrical surface of each pillar and wired to make up a Wheatstone bridge as may be seen in Fig. 4a. Maximum bridge output is attainable because the strain gauges are specifically disposed perpendicular to each other on each side of the pillar, to take full advantage of the Poisson effect on the axially loaded pillars.

The radial load pillars were calibrated in a universal tensile-test machine before final fixing to the bedplate (2), the output from each bridge (load pillar) being monitored in the data acquisition system. Thus radial loads can be continuously monitored throughout any test. Loads were applied incrementally and decrementally and the

corresponding outputs were recorded. The procedure was repeated several times. The results gave a linear response with excellent repeatability. Hysteresis was negligible (less than 1%).

3.2. Axial loading

Axial preload is applied to the twin taper roller bearing system via a finely-threaded nut (9) on the test shaft (13), Fig. 2. A brass ring (10) mounted between the axial loading nut (9) and the inner ring of the left tapered roller bearing (11) is used for measuring the axial preload. This ring, as may be seen in Fig. 4b, carries a strain-gauge bridge and was previously calibrated before being mounted on the test shaft. It was appreciated that inherent friction would be present in the contact between the taper roller bearing inner ring and its seating. To circumvent this effect pressurized oil was injected between the surfaces when applying the axial preload to the twin taper roller bearings.

Calibration of the axial load ring was performed on a universal compression-test machine. The procedure was identical to that employed for the calibration of the radial load pillars, except that compressive axial load, rather than tensile load, was applied to the ring.

3.3. Torque measurement system

Basically the measurement of a test-bearing operating torque is performed by measuring a force at a radial distance from the shaft centre-line.

The torque measurement system shown in Fig. 5 consists of two load-cells (5) and (8) positioned opposite to each other (relative to the test-shaft) and two torque-arms (6) and (7) attached to the torque-tube (2).

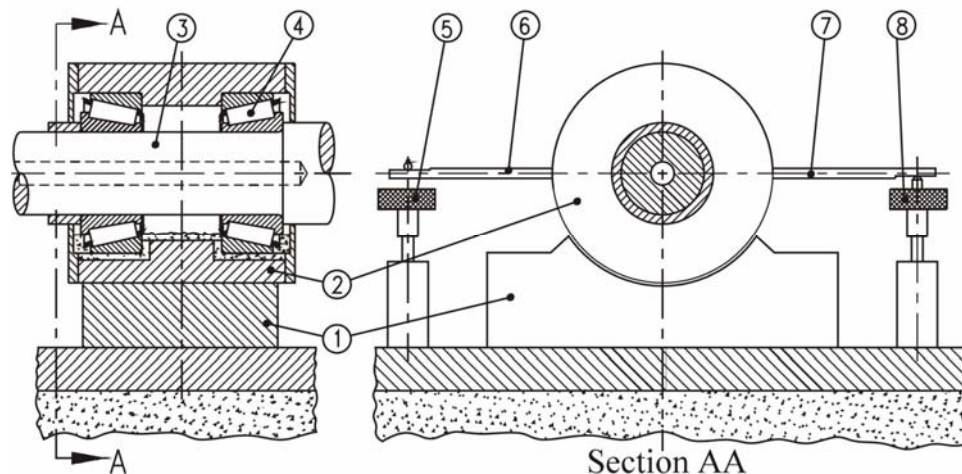


Figure 5. Torque measurement system

A high pressure hydraulic-pump provides SAE20 oil to the hydrostatic bearing (1), such that an oil film of constant thickness is maintained between the torque-tube and the hydrostatic block. Metal-to-metal contact between the torque tube and the hydrostatic block is therefore avoided. Thus, rotation of the test-shaft (3) would cause the torque-tube to rotate in the same direction due to the action of the test bearing's friction torque. However, as shown in Fig. 5, rotation of the torque-tube is constrained by the twin torque arms (6) and (7) and the push/pull load-cells (5) and (8).

The product of the semi-sum of the vertical forces measured by the load-cells (5) and (8) and the distance from each other gives the tapered roller bearings friction torque, which can be continuously monitored throughout any test.

The components of a 'pull' type load-cell are shown in Fig. 6a. The load-cells are high sensitivity units, consisted by a cruciform member of Beryllium/copper carrying a strain-gauge bridge. The assembly is mounted in a brass housing threaded to allow vertical adjustment, as can be seen in Fig. 6b, which shows the cross-section and the top view of a push load-cell, with the cover removed, for clarity.

It was appreciated that for a load direction as shown in Fig. 6b, the top surface of the cruciform arms are in compression near the centre and in tension near the end. The strain gauges were therefore bonded to the cruciform arms according to the particular arrangement shown in Fig. 6b. This arrangement, in combination with a specific strain gauge wiring, provides a bridge output greater than that attainable if the four strain gauges were equidistant from the cruciform centre.

The push load-cells were specifically calibrated by using an apparatus consisted by a simply supported beam; a piece of cylindrical rod supported at one end by a knife-edge and at the other end by the load cell loading column. This latter contact was, in fact, maintained between the ball bearing glued to the top of the load column (see Fig. 6) and a flat end on the cylindrical rod. A load hook was placed at the centre of the beam, allowing weights to be hung.

The pull load cell was calibrated by using a string and pulley device, one end of the string being attached to the load cell cruciform holed center shown in Fig. 6a, and the other supporting increasing weights.

Initially the outputs from the load-cells were set to zero, under unloaded conditions, by adjusting the ‘bridge balancing’ unit. Load was then applied to the load-cells in increments and decrements, the corresponding outputs being recorded in the data acquisition system. Hysteresis was insignificant for the two load-cells (less than 1.5%).

Calibrations were repeated at various laboratory temperatures and the load-cell outputs were found to be insensitive to temperature effects.

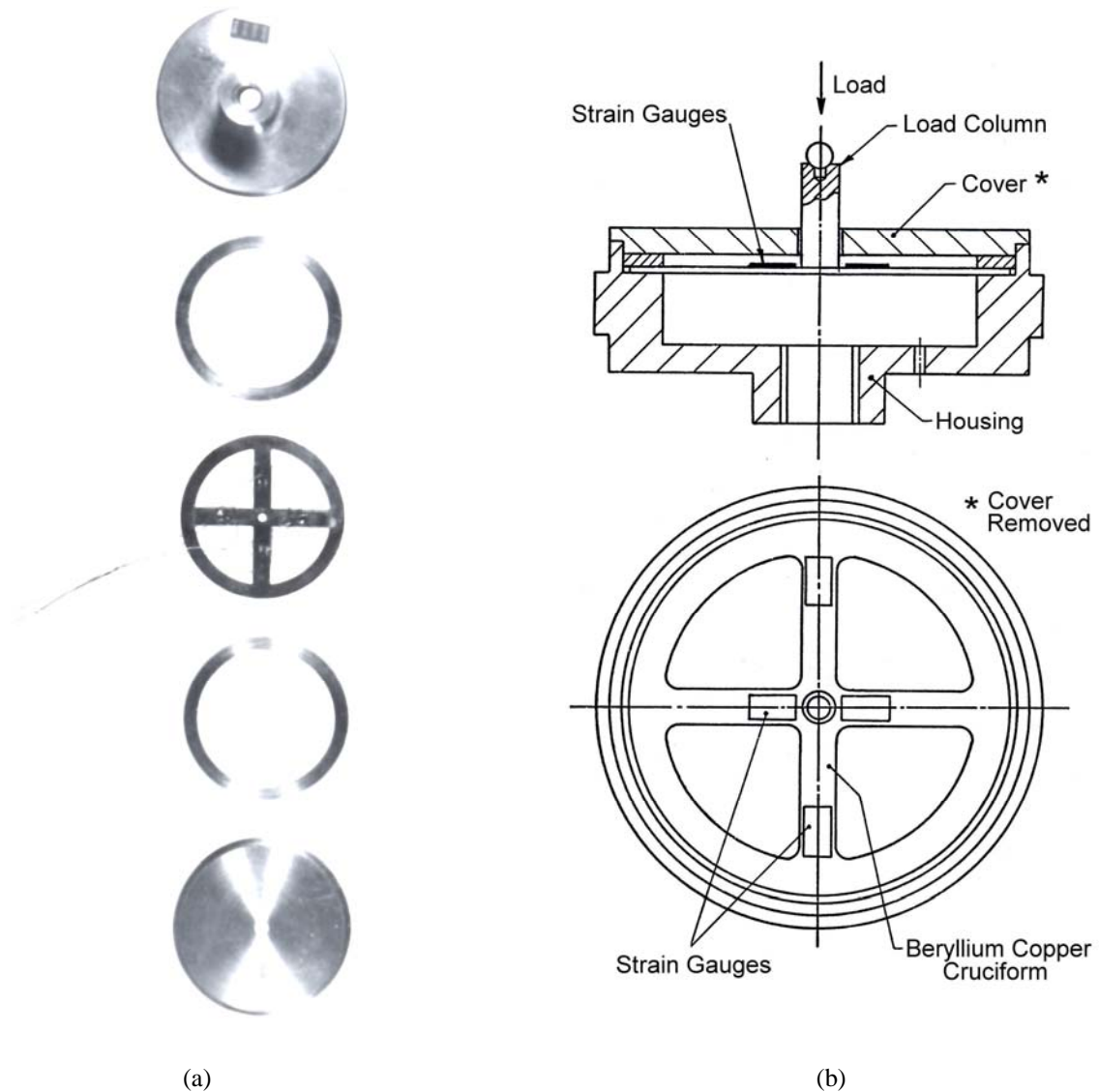


Figure 6. Pull load cell components (a) and the push load cell showing the cruciform with strain-gauges (b)

3.4. Temperature measurement

Temperature measurement throughout the tests was accomplished by employing thermocouples embedded at several points within the test module, including the test shaft, bearing housing, the test bearings proper, the hydrostatic block and the bedplate.

All the thermocouples were manufactured from varnish-coated 0.13mm diameter chromel/constantan wires. Figure 7a shows the construction stages involved for manufacturing a typical thermocouple. Firstly, the varnish coating is removed from the ends of both wires for a length of about 5mm. Both wires are then passed separately through the twin holes of a short length (approx. 3mm) of ceramic outgassing tube, in such a way that about 4mm are left protruding. The second stage consists of twisting the protruding wires together. The wires are then cut, leaving approximately 2mm protruding which are then spot-welded to form a bead. The wires are housed in a P.T.F.E. sheath, thereby giving the wires protection from short-circuit effects. Since the ceramic tube is friable the couple end is protected by housing it in a 17 SWG hypodermic tube, shown in Fig. 7a.

Thermocouples for measuring the temperatures of non-rotating points of the assembly were manufactured with longer wires, allowing for direct connection with the data acquisition system.

For the assessment of the inner and outer raceways temperatures together with the guide flange lip temperature, thermocouples were inserted into spark-eroded holes drilled through the back or the side of the rings. For example, as can be seen in Fig. 7b, which shows the bearing inner ring with two holes at the guide flange and the inner race for insertion of the corresponding thermocouples.

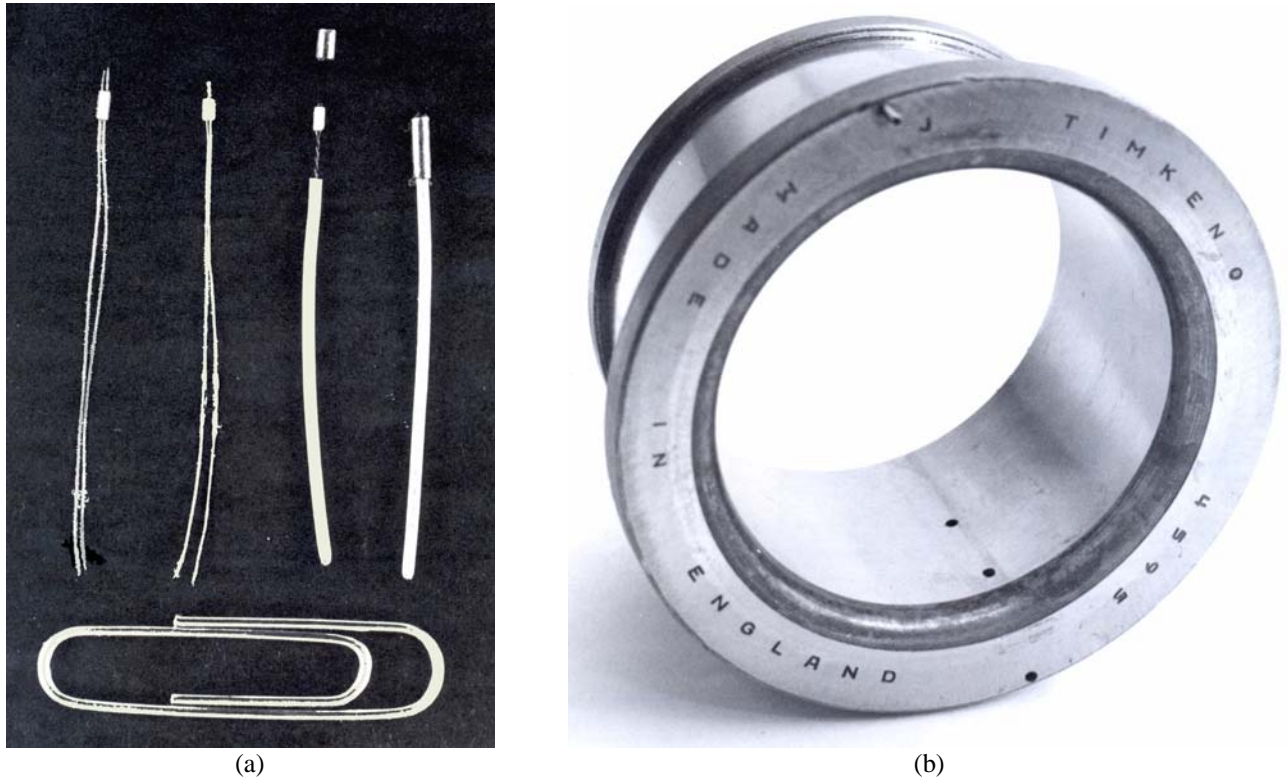


Figure 7. Thermocouple manufacturing sequence (a); inner ring with spark- eroded holes for thermocouples (b).

Mounting thermocouples in the inner rings of the tapered roller test bearing was a somewhat delicate operation, according to the following steps:

- 1) Disassemble the cone by separating the inner ring from the rollers and cage.
- 2) Drill holes for mounting thermocouples as shown in Fig. 7b.
- 3) Cement the thermocouples in position, using an Epoxy-Resin adhesive.
- 4) Reassemble the cone by mounting the cage with rollers on the inner ring.

5) Slide the cone to its final position on the shaft, care being taken to ensure that the thermocouple wires were free to slide in a keyway on the shaft.

The inner rings and shaft thermocouple wires were connected to a high-quality silver/silver-graphite slip ring unit, through an axial hole drilled within the shaft, and from that unit to the data acquisition system.

Air cooling was used to maintain the slip rings at a constant temperature during the tests. 'Seebeck' effects were alleviated by mounting rotating junctions on a junction disc integral with the shaft and rotating in ambient air.

The slip rings were drive by the test shaft through a specially designed flexible coupling, the whole unit being located on the front bearing housing by a three arm mounting bracket secured to that housing by three cylindrical pillars. The arrangement may be seen in Fig. 1.

The outer rings of the test bearings were press-fitted to the corresponding housings (or sleeves). Special care was taken to obtain alignment between each spark-eroded radial hole in the bearing outer ring and the corresponding hole drilled through the housing wall. Both holes had been drilled prior to fitting, the housing holes being slightly larger in diameter than the outer ring holes. The thermocouple beads were introduced through the aligned holes and cemented into position, the fitting procedure being similar to the inner-ring thermocouples.

No problem was anticipated with the thermocouples directly connected to the data acquisition system since there are no secondary junctions for such thermocouple circuits.

However, rotating thermocouples require the use of a slip ring assembly, and this introduces additional bimetal junctions into the thermocouple circuit. Therefore, to minimize any consequential errors, the following conditions are required, on the basis of Fig. 8

- a) Junction 2-4 (Chromel-Silver) is equal to junction 12 (Silver-Chromel)

- b) Junction 3-5 (Constantan-Silver) is equal to junction 13 (Silver-Constantan)
- c) Junction 8 (rubbing junction between the silver ring and the silver-graphite brush on the chromel side) is equal to junction 9 (rubbing junction on the Constantan side of the circuit).

The conditions 'a' and 'b' are accomplished by maintaining those junctions at the same temperature, whilst the condition 'c' is fulfilled by the manufacturers by supplying the slip ring unit with all the rings and brushes of the assembly similar, such that any voltage generated by rubbing surfaces would be of equal magnitude.

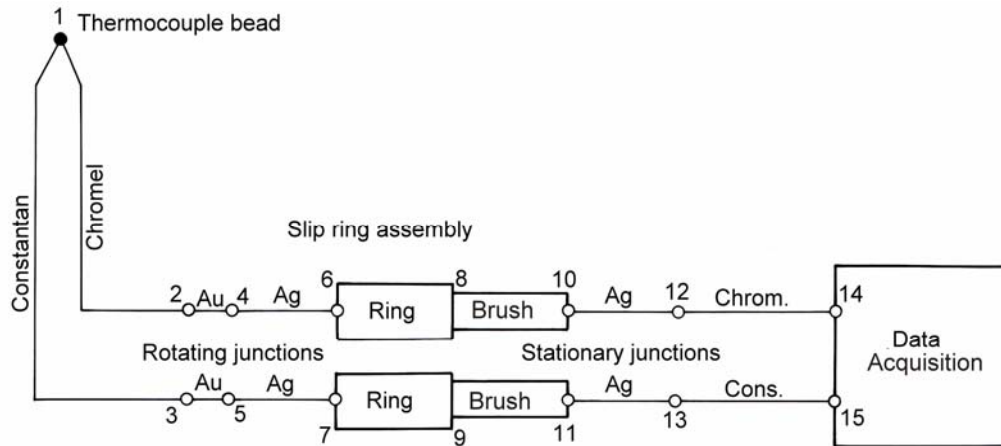


Figure 8. Rotating thermocouple simulated circuit

4. The test bearings.

Two identical taper roller bearings ‘Timken 4595/4536’ were employed, these being mounted back-to-back (indirect mounting) in the central sleeve (see Fig. 2). As can be seen in Fig. 9, the bearing is of separable design, i.e. the rollers, cage and inner ring assembly (cone) and the outer ring (cup) are mounted separately to the shaft and housing respectively, in any machine device.

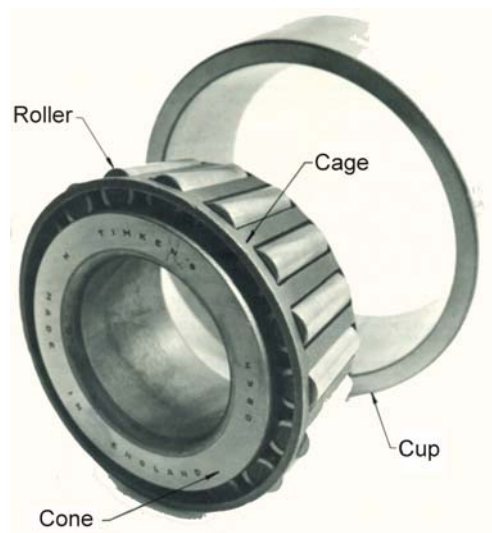


Figure 9. The test bearing with the cup partially removed

The bearing design is such that, under proper operating conditions, all the components carry the load, with the exception of the cage, whose primary function is to space the rollers around the inner ring. The rollers and races operate under pure rolling motion as a result of the design principle: the apices of the tapered surfaces meet at a common point on the bearing axis, as shown in Fig. 10. However, sliding contact takes place between the roller large end and the flange on the cone. A spherical surface of radius equal to 97% of the apex length is ground on the roller large end, such that under no load, a point contact is established between that roller end and the cone rib. Under load this contact becomes elliptical, allowing the formation of a lubricant film on the contact area, as shown by Cretu et al (1995), Zhou and Hoeprieh (1991), Wang et al (1996) and Wren and Moyer (1972).

Owing to the tapered races, the bearing is particularly suitable for carrying combined (radial and thrust) loads. However, single-row tapered roller bearings can carry thrust loads in one direction only. A radial load applied to the bearing gives rise to an induced axial load which must be counteracted and the bearing is therefore generally mounted against a second tapered roller bearing, as shown in Fig. 2.

The main characteristics of the test bearings are resumed in Tab. 1, dimensions being given in millimeters, even though the bearing is a inch series, as shown in Fig. 10.

Table 1. The test bearing characteristics (dimensions: mm)

Serial number	Diameter		Cup contact angle	Roller diameter	Roller length	Number of rollers
	Inner	outer				
Timken 4595/4596	53.975	111.125	12,75°	11.43 (mean)	29.970	17

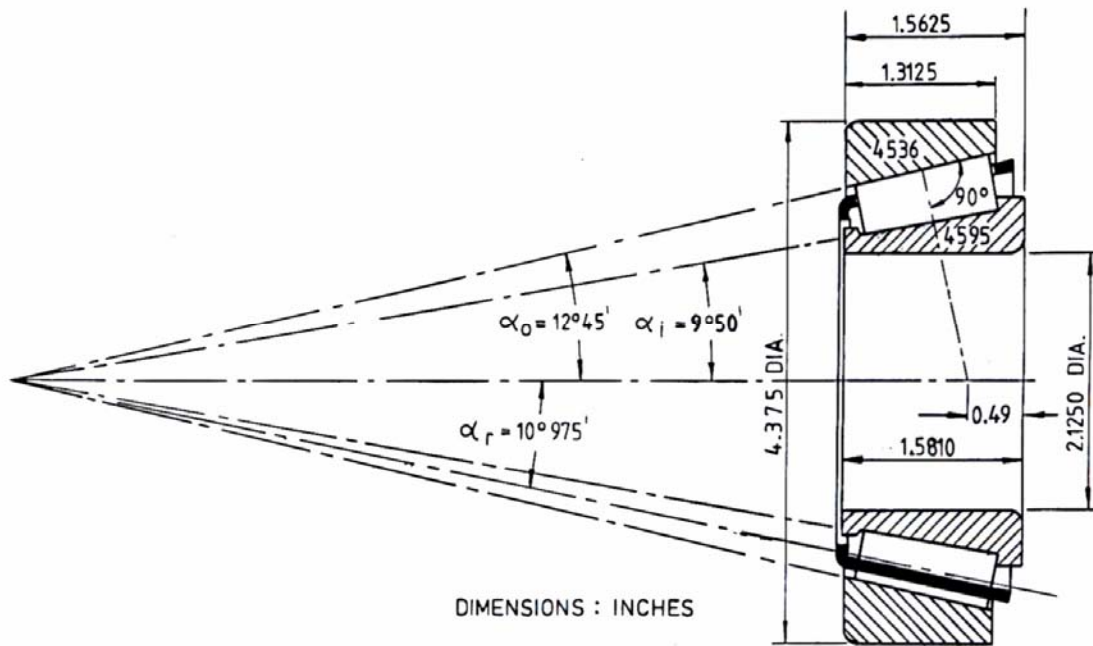


Figure 10. Taper roller bearing ‘Timken 4595/4536’

5. Experimental results and discussion.

As shown in Fig. 11, a large number of thermocouples was embedded at strategic points on the housing and shaft, particularly at the housing base (hydrostatic block) and bedplate. This procedure allows for the assessment of the temperature gradient and therefore heat dissipation rates through these parts of the bearing assembly.

Progressive ‘running-in’ of the test bearings was achieved through a gradually increasing duty cycle of speed and load, experimental results being taken only after the running-in period.

For each loading condition, the shaft speed was varied usually from 500 to 5000 rpm, in steps of 500 rpm. Thermal equilibrium for the whole assembly established itself after 3-4 hours, for the initial speed. A further hour was necessary after each speed increment to re-establish thermal equilibrium.

Steady state temperatures and torque are the subject of the present study, therefore, data was recorded only after thermal stabilization of the system, for each specific operating condition of load, speed and lubrication.

Figure 11 shows the temperature distribution within the tapered roller bearings assembly, for a 4000 N radial load and a 4000 rpm rotational speed, the bearings being bath lubricated by a SAE 20 oil. Note the difference between the outer raceway temperature of 105.2°C at the higher position in the vertical mid plane and 103.3°C at the level of the shaft axis. It is also important to observe the significant temperature gradients found in the lower part of the housing, i.e., the hydrostatic block. Calculations based on those values (by using standard equations for heat transfer by conduction) showed that some 35-45% of the total heat generated is dissipated in this way. This is due to more material and surfaces for conductive and convective heat transfer rate at the lower part of the whole bearing assembly As can also be seen from the figure, the outer race temperature at the level of the shaft axis was about 2% lower than the inner race temperature and 1% higher than the guide flange lip temperature.

The corresponding measured friction torque was equal to 1.14 N.m, i.e., 0.57 N.m for each tapered roller bearing, assuming an equal distribution from both bearings.

With a view to simulate the central bearing assembly to that of an ordinary bearing housing, a few tests were carried out without oil flow between the hydrostatic bearing surfaces. It was observed that the operating temperatures of the test bearing proper was less than 3% higher than those for the case of oil flow between the hydrostatic bearing surfaces. The hydrostatic block temperatures were, however, about 12% higher than those for the latter case. It can be concluded, therefore, that the heat 'take-up' by the hydrostatic bearing oil is approximately compensated by the increased rate of heat conducted to the hydrostatic block (and from there to the bedplate), when there is no oil flow between the hydrostatic bearing surfaces. For this situation, calculations based on the temperature gradients measured in the lower part of the bearing housing showed that 58-67% of the heat generated in the bearing is conducted out of the bearing from the housing base to the bedplate.

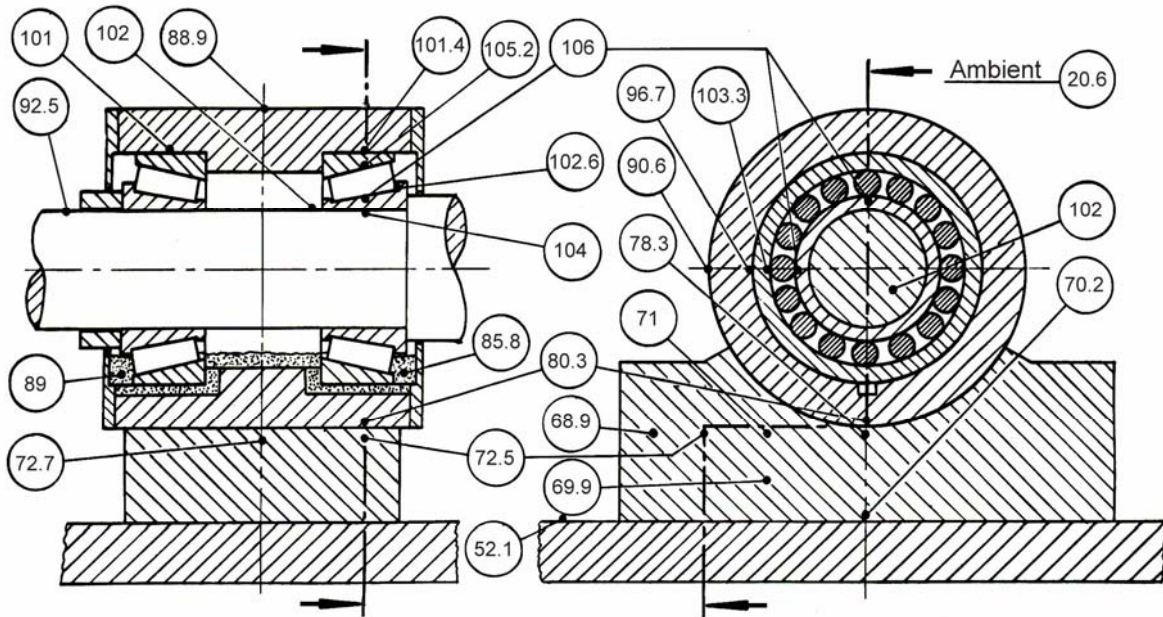


Figure 11. Temperature distribution within the bearing assembly, for a 4000 rpm speed, and a 4 kN radial load

Figure 12 shows the variation of the inner race and the guide flange lip temperatures and the steady state friction torque of one of the tapered roller bearings with rotational speed, for a SAE 20 oil and a 4000 N radial load.

It may be seen that the temperatures increase almost linearly with speed, the guide flange lip temperature at the roller end contacts being about 2 to 4°C lower than the inner race temperature.

Initially, the bearing friction torque increased almost linearly with speed, in the range from 1000 to 2600 rpm, then, due to the significant decrease of the oil viscosity with temperature, the bearing friction torque remained almost constant from about 2600 to 3000 rpm and then decreased for speeds above 3000 rpm.

This torque behaviour is different in comparison to the experimental and theoretical results found in the literature, showing a friction torque varying almost linearly with speed, for the total speed range. For example, for both a larger and a smaller tapered roller bearing, the experimental results presented by Zhou and Hoeprich (1991) and also by Cretu et al (1995) show a bearing friction torque with a small almost linear increase with rotational speed in the range from 1000 to 4000 rpm. The same viscosity grade (SAE 20) was used for the fully flooded lubrication condition under which their tests were carried out.

For the smaller bearing, Timken LM12700, with inner and outer diameters equal to 22 and 46mm, respectively, and a 41,5mm cup work point diameter, the experimental bearing friction torque presented by Cretu et al (1995), for a 3000 rpm rotational speed was about 5.9 times lower than the 0.6 N.m friction torque shown in Fig. 11, for the test bearing of the present paper, which has a cup work point diameter of about 96mm. On the other hand, for a larger bearing, not specified in Cretu's paper, but with 120mm cup work point diameter, the experimental torque presented by Cretu for the same rotational speed and the same oil viscosity grade (SAE 20) was about 4.14 times higher than the 0.6N.m shown in Fig. 11 for the Timken 4536/4595 tapered bearing of the present paper.

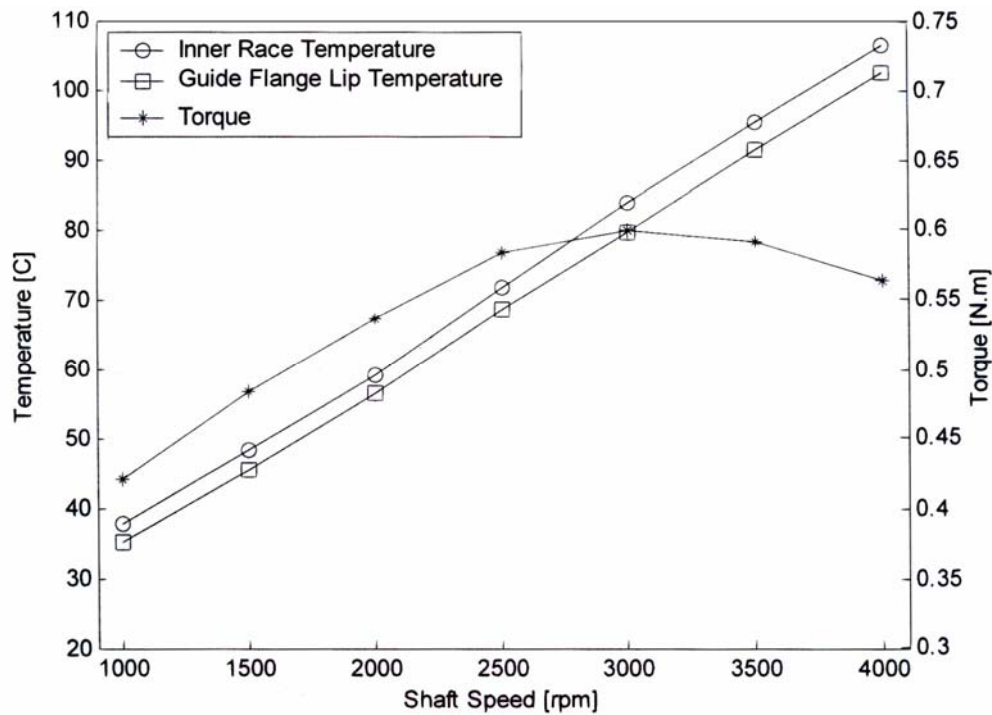


Figure 12: Temperature and friction torque of one of the tapered roller bearings versus rotational speed

6. Conclusions

A full description of the test rig and instrumentation for an experimental analysis of a twin tapered roller bearing assembly has been presented.

The tests were carried out for various conditions of load and rotational speed. Generally, for a given condition of load and by varying the rotational speeds, and after thermal stabilization, it was observed that the bearing friction torque initially increased with speed in the range from 1000 to 2500 rpm, remained almost constant for the speed range from about 2600 to 3000 and then started to show a small decrease for speeds higher than about 3000 rpm. As expected, the steady state temperatures increased almost linearly with speed and with load, the inner raceway temperature being about 2 to 4% higher than that of the outer raceway.

From the temperature gradient measured at the housing base, it was concluded that heat dissipation by conduction to the bedplate is of significative importance to dissipate the heat generated in the bearing.

7. References

- Cretu, S., Mitu, N. and Bercea, I., 1995, "A dynamic analysis of tapered roller bearings under fully flooded conditions", *Wear* 188, Elsevier, pp. 11-18.
- Parker, R.J., and Signer, H.R., 1978, "Lubrication of high-speed, large bore, tapered-roller bearings", *Journal of Lubrication Technology, ASME Trans.*, Vol. 100, pp. 31-38.
- Wang, W., Wong, P.L. and Zhang, Z., 1996, "Partial EHL analysis of rib-roller end contact in tapered roller bearings", *Tribology International, Elsevier*, Vol. 29, No. 4, pp. 313-321.
- Wren, F.J. and Moyer, C.A., 1972, "Understanding friction and E.H.L. films in concentrated contacts of a tapered roller bearing", *Elastohydrodynamic Lubrication*, pp. 55-60, *Instn. Mech. E.*, C10/72, London.
- Zhou, R.S. and Hoeprich, M.R., 1991, "Torque of Tapered Roller Bearings", *Journal of Tribology, ASME Transactions*, vol. 113, pp. 590-59.